



**HAL**  
open science

# Stability of ablation flows in inertial confinement fusion: non-modal effects

G Varillon, J.-M Clarisse, A. Couairon

► **To cite this version:**

G Varillon, J.-M Clarisse, A. Couairon. Stability of ablation flows in inertial confinement fusion: non-modal effects. 2020. hal-02892019v3

**HAL Id: hal-02892019**

**<https://polytechnique.hal.science/hal-02892019v3>**

Preprint submitted on 2 Nov 2020 (v3), last revised 15 Jan 2021 (v4)

**HAL** is a multi-disciplinary open access archive for the deposit and dissemination of scientific research documents, whether they are published or not. The documents may come from teaching and research institutions in France or abroad, or from public or private research centers.

L'archive ouverte pluridisciplinaire **HAL**, est destinée au dépôt et à la diffusion de documents scientifiques de niveau recherche, publiés ou non, émanant des établissements d'enseignement et de recherche français ou étrangers, des laboratoires publics ou privés.

# Stability of ablation flows in inertial confinement fusion: non-modal effects

G. Varillon,<sup>1,2</sup> J.-M. Clarisse,<sup>1</sup> and A. Couairon<sup>2</sup>

<sup>1</sup>CEA, DAM, DIF, F-91297 Arpajon, France

<sup>2</sup>CPHT, CNRS, Ecole Polytechnique, Institut Polytechnique de Paris, Route de Saclay, 91128 Palaiseau, France\*

(Dated: November 2, 2020)

Fast transient growth of hydrodynamic perturbations due to non-modal effects is shown to be possible in an ablation flow relevant to inertial confinement fusion (ICF). Likely to arise in capsule ablaters with material inhomogeneities, such growths appear to be too fast to be detected by existing measurement techniques, cannot be predicted by any of the methods previously used for studying hydrodynamic instabilities in ICF, yet could cause early transitions to nonlinear regimes. These findings call for reconsidering the stability of ICF flows within the framework of non-modal stability theory.

PACS numbers:

Inertial confinement fusion (ICF) has been proposed some 50 years ago as a viable means for harnessing thermonuclear fusion with the aim of producing energy. This scheme relies on the irradiation of spherical capsules of millimeter size, filled with thermonuclear fuel, at high energy fluxes capable of producing, over nanoseconds, a fuel compression of thousands of times solid density [1]. Such high compressions critically depend, however, on a mitigation of hydrodynamic instabilities during capsule implosion, since these may hamper the compression and heating of the fuel, possibly ruining the whole process. In particular, the subsonic heat-wave flow, or *ablation flow*, that results from the irradiation of the outer layer, the *ablator*, of a fusion capsule and drives its implosion, was right away considered as a dominant factor of hydrodynamic perturbation growth [2, 3]. Despite several decades of dedicated numerical simulations, experiments, theoretical works and improvements in the understanding, prediction and mitigation of capsule implosion perturbations, ICF is still in practice impeded by issues of hydrodynamic instability (e.g. Refs. 4–6).

The strongly compressible, nonuniform and unsteady nature of capsule implosions, besides the complexity of the high-temperature physics at stake, renders the study of their hydrodynamic stability especially arduous. Two types of approaches have then been pursued: (i) stability analyses using simplified physical modelings and (ii) computations of perturbation amplifications trying to be as realistic as possible. The framework of compressible inviscid fluid dynamics with nonlinear heat conduction has undoubtedly contributed to a better understanding of ablation flow instabilities (cf. the review of Ref. 7). Corresponding stability analyses have exclusively consisted in applying the method of normal modes, or *modal stability analysis*, for idealized reduced portions of the implosion flow (e.g. steady, quasi-isobaric, constantly accelerated, at times discontinuous, ablation flows) or more realistic, i.e. simulated, flows under the frozen-time assumption. Such analyses, since they focus on the least stable eigenmode of the flow, can only yield asymptotic sta-

bility results and are inevitably, given the implosion unsteadiness, of restricted validity in time and perturbation wavenumber ranges. Perturbation amplification computations belong to a different approach, sometimes called *amplification theory* (AT), which consists in computing responses of an arbitrary base flow, solution to an initial and boundary value problem (IBVP), to selected initial and/or boundary perturbations. Such computations are not sufficient by themselves for obtaining results of stability. Nevertheless, this approach has been widespread in ICF, especially using multi-dimensional hydrodynamics codes dedicated to ICF physics since the restrictive settings of theoretical models are thus avoided.

Yet another approach exists that has never been considered in ICF and which consists in applying methods of *non-modal stability theory* [8], the sole capable of giving stability results for unsteady flows, irrespective of time horizons. However, given available computational means, the task is daunting for a complete capsule implosion and it is therefore logical to start with a simpler flow. In this Letter, we initiate this effort by performing a non-modal stability analysis of an unsteady ablation flow modeling the early stage of a capsule implosion.

Confidence in the ability of ICF hydrodynamics codes to reproduce instability dynamics has been progressively built through comparisons between AT computations and specifically designed experiments where a dominant, i.e. considered most detrimental, perturbation source is selected by carefully controlling experimental conditions (e.g. Refs. 9, 10). However, AT computations, carried out with these very codes, still display unexplained discrepancies with ablation experiments on capsule ablaters at standard specifications for fusion [11, 12]. The short history of ICF has shown that, among the many possible explanations, overlooking some perturbation sources or unappreciated effects is highest in the list [6, Sec. V]. For several decades, based on modal stability analyses, AT computations and dedicated experiments, roughness of the ablator surfaces was considered as the most detrimental perturbation source. Intensive efforts were spent

on this issue, leading to surface finish requirements for fusion. By then ablator material inhomogeneities were thought to play a minor role. This way of thinking was turned around by the experiments of Ref. [11]: ablator inhomogeneities could be in fact a major perturbation source [13]. In such experiments [11, 12], many perturbation sources are competing, without an artificial dominance of one on the others, and the characterization of their initial or temporal contributions is insufficient for setting up representative enough AT computations. Besides, it is known that perturbation eigenmodes that are stable according to modal stability theory can induce, through their interaction, perturbation transient growth [14]. Hence different perturbation sources—even though each of them, separately, are identified to be minor—could lead, upon proper combination, to perturbation amplification. Modal stability theory, by assuming that eigenmodes are orthogonal, ignores such interactions, or *non-modal effects*. In principle, AT computations could capture such growths provided that they are started from appropriate initial conditions. However, identifying systematically these most detrimental initial perturbations requires the use of methods that have never been considered in ICF. The alternative—a brute force use of AT computations for sampling the space of eligible initial conditions so as to, hopefully, find those leading to maximum amplification—is at best unrealistic. Therefore a genuine risk exists of missing the most detrimental perturbation sources due to a lack of a proper methodology.

Non-modal stability theory precisely furnishes such a methodology by fully exploiting the fact that the finite-time dynamics of a system is not only ruled by the eigenvalues of its evolution operator but also by this operator eigenmodes [15]. Elaborated over the last thirty years, this theory has been successful in elucidating some withstanding problems in hydrodynamic stability [8]. Until proven otherwise, non-modal effects and associated transient growths cannot be ruled out nor held as negligible in ICF ablation flows. By performing a linear non-modal analysis, local in space and time, we address the questions (i) of whether or not an ICF ablation wave may present non-modal effects, and (ii) of the associated mechanism(s) of transient growth.

The present stability analysis is conducted on a self-similar ablation flow in slab symmetry representative of the early stage of an ICF capsule implosion [16–19]. Such a flow presents the essential features of the subsonic heat wave that prevails within the capsule ablator during this stage of the implosion (compressibility, stratification, unsteadiness), including its whole structure (Fig. 1): (i) a leading shock front, (ii) a quasi-isentropic compression region, (iii) an ablation layer, and (iv) an expansion wave where heat conduction dominates (‘conduction region’). A dimensionless formulation of the equations of motion is retained so as to keep the flow description as general

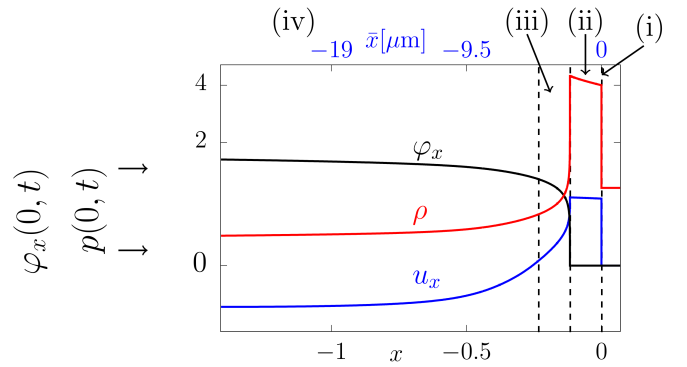


FIG. 1: Self-similar ablation-wave solution to Eq. (1) for  $\gamma = 5/3$ ,  $(\mu, \nu) = (2, 13/2)$  and boundary condition parameters  $(\mathcal{B}_\phi, \mathcal{B}_p) = (0.8, 0.31)$ . Dimensionless spatial profiles in the coordinate  $x$  at time  $t_0 = 1$  of the fluid density  $\rho$ , longitudinal velocity  $v_x$  and heat flux  $\varphi_x$ . Correspondence with the actual physical extent of the wave, relative to the shock front, at the chosen reference time of a simulated capsule implosion is also indicated (top axis)<sup>a</sup>.

<sup>a</sup>See Supplemental Material, Sec. I.

as possible [18, 20]. For one-dimensional motion along the  $x$ -axis of a Cartesian coordinate system  $(O, x, y, z)$ , the equations of motion, written in the Lagrangian coordinate  $m$  where  $dm = \rho dx$ , come as

$$\begin{aligned} \partial_t(1/\rho) - \partial_m v_x &= 0, & \partial_t v_x + \partial_m p &= 0, \\ \partial_t(C_v T + v_x^2/2) + \partial_m(pv_x + \varphi_x) &= 0, \end{aligned} \quad (1)$$

where  $\rho$ ,  $v_x$ ,  $p$ ,  $T$ ,  $\varphi_x$  denote, respectively, the fluid density, velocity, pressure, temperature and heat flux as functions of  $(m, t)$ . The dimensionless equation of state for a polytropic gas,  $p = \rho T$ , with  $C_v = 1/(\gamma - 1)$ ,  $\gamma$  being the fluid adiabatic exponent, and the heat-flux expression  $\varphi_x = -\rho^{-\mu} T^\nu \rho \partial_m T$ ,  $\mu \geq 0$ ,  $\nu > 1$ , supplement this system. Self-similar reductions of Eq. (1) arise when a semi-infinite slab ( $m \geq 0$ ), initially at rest and perfectly cold, is subject to particular time-power laws for the incident heat-flux and pressure at the material external surface  $m = 0$ . (More details are given in the Supplemental Material accompanying this Letter [24].)

The stability of flows ruled by Eq. (1) is studied using an Eulerian description of three-dimensional linear perturbations in the coordinate system  $(x, y, z)$ . Once expressed with the Lagrangian coordinate  $m$  and Fourier transformed in the variables  $(y, z)$ , the corresponding system of governing partial differential equations [25] reads in vector form

$$\partial_t \widehat{\mathbf{U}} = \mathcal{A}(m, t, \partial_{m\cdot}, k_\perp) \widehat{\mathbf{U}}, \quad \widehat{\mathbf{U}} = (\widehat{\rho} \widehat{v}_x \widehat{d}_\perp \widehat{T})^\top, \quad (2)$$

for the  $yz$ -Fourier components:  $\widehat{f}$ , of the perturbations of the base flow variables  $f = \rho, v_x, T$ , and  $\widehat{d}_\perp$ , of the transverse divergence of the transverse velocity perturbation. The perturbation evolution operator,  $\mathcal{A}$ , depends

on space, time and the wavenumber  $k_{\perp} = \sqrt{k_y^2 + k_z^2}$ . Perturbation boundary conditions at the geometrically deformed external surface (es)  $m = 0$  and shock front (sf)  $m = m_{\text{sf}}(t)$  complete this system [26].

The possibility of perturbation short-time growth for the self-similar ablation wave of Fig. 1 is investigated by means of a local analysis, in time and space, of Eq. (2). In effect, for some reference time  $t_0 > 0$  and at any location  $x_* = x(m_*, t_0)$  within the wave extent, we consider perturbations of longitudinal characteristic lengths that are shorter than the smallest local gradient length of the flow, say  $l_{\nabla}(x_*)$ . Under this assumption the operator  $\mathcal{A}|_{t_0}$  may be held as uniform over a neighborhood of  $x_*$ , reducing the analysis of Eq. (2) to that of the  $m$ -Fourier transform of  $\mathcal{A}|_{t_0}$ , say  $\mathcal{A}_0$ , under the condition  $\varkappa_x(x_*) \equiv \rho(x_*) k_m l_{\nabla}(x_*) \gg 1$  bearing on the longitudinal wavenumber  $k_m$ . Perturbation transient growth is then assessed by computing the maximum instantaneous growth rate  $\sigma_0(k_m, k_{\perp})$  [27] of a global norm of  $\hat{\mathbf{U}}$  [28], i.e.

$$\sigma_0(k_m, k_{\perp}) \equiv \max_{\tilde{\mathbf{U}}_*} \left( \frac{1}{\|\tilde{\mathbf{U}}_*\|^2} \frac{d\|\tilde{\mathbf{U}}_*\|^2}{dt} \right) \Big|_{t_0}, \quad (3)$$

where  $\tilde{\mathbf{U}}_*$  stands for the  $m$ -Fourier component of the restriction of  $\hat{\mathbf{U}}$  to a neighborhood of  $m_*$ . Such computations [21] are carried out for  $m_*$  covering the whole extent of the ablation wave, for ranges of  $k_m$  such that  $\varkappa_x(x_*) \geq 10$ , and for different values of  $k_{\perp}$ . Maps of  $\sigma_0$  as a function of the flow location  $x_*$  and of the normalized longitudinal wavenumber  $\varkappa_x$  are thus obtained (Fig. 2). Regions of non-modal growth, i.e. regions of modal stability but with positive  $\sigma_0$  [29], are identified (colored areas in Fig. 2) and distinguished from regions of modal instability [30] (black areas). Sizable portions of the conduction region ( $-1.15 \lesssim x \lesssim -0.12$ ), the ablation layer ( $x \approx -0.12$ ), for extended ranges of  $\varkappa_x$ , and the compression region ( $-0.12 < x < 0$ ), for restricted  $\varkappa_x$ , are prone to non-modal growth. This analysis shows that locally the perturbation evolution operator for an ablation wave driven by nonlinear heat conduction is non normal for a wide range of perturbation characteristic lengths [31]. This finding implies that the method of normal modes is insufficient for assessing the stability property of such a flow and that perturbation transient amplifications have to be taken into account and therefore searched for.

The actual occurrence of non-modal growth is confirmed by means of AT computations of  $\hat{\mathbf{U}}$  by solving Eq. (2) for  $t \geq t_0 = 1$  with the aforementioned boundary conditions at the external surface and shock front [32]. Initial conditions, inferred from the above non-modal stability analysis, are defined as

$$\hat{\mathbf{U}}(m, t_0, k_{\perp}) = w(m, k_m) \text{Re}(\tilde{\mathbf{U}}_0^{\text{opt}}(m_*, k_m, k_{\perp}) e^{ik_m m}), \quad (4)$$

where  $w$  is a specifically chosen mask function, sufficiently smooth and non-zero over a limited domain cen-

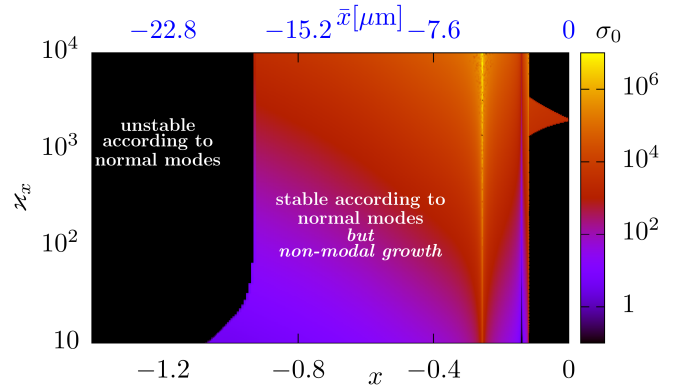


FIG. 2: Intensity map, in the plane  $(x, \varkappa_x)$ , of  $\log \sigma_0$ ,  $\sigma_0 > 0$ , obtained from Eq. (3) for  $k_{\perp} = 1.2$ : regions of non-modal growth but modal stability (color) and regions of modal instability (black). Same horizontal axis conventions as in Fig. 1.

tered about  $m = m_*$ . The function  $\tilde{\mathbf{U}}_0^{\text{opt}}$  is the principal eigenmode of the operator  $(\mathcal{A}_0 + \mathcal{A}_0^{\dagger})$ ,  $\mathcal{A}_0^{\dagger}$  denoting the adjoint operator of  $\mathcal{A}_0$ —i.e. the optimal-growth initial condition yielding the maximum growth rate (3). Results obtained at a location within the compression region for normalized wavenumbers  $\varkappa_x$ ,  $\varkappa_{\perp} = k_{\perp} l_{\nabla}(x_*)$  for which the method of normal mode predicts stability, are exemplified in Table I(a) and illustrated in Figs. 3 and 4. Growth rates  $\sigma_{\text{AT}}$ , extracted from AT computations with initial conditions (4), are in good agreement with the values of  $\sigma_0(k_m, k_{\perp})$  given by Eq. (3). This agreement and growth times,  $\sigma_{\text{AT}}^{-1}$ , much smaller than the base-flow characteristic time, here  $t \approx 1$ , validate the local analysis leading to Eq. (3). Through these simulations, initial transient growth is verified at flow locations where modal stability analysis predicts decaying perturbations, thus substantiating the reality of local non-modal effects in a typical ablation flow.

TABLE I: (a) Characteristic growth times:  $\sigma_0^{-1}$  ‘predicted’ via Eq. (3) for the flow location  $x_* = -0.06$ , and  $\sigma_{\text{AT}}^{-1}$  extracted from AT computations. (b) Corresponding values obtained for the chosen reference time of a simulated capsule implosion<sup>a</sup> at the equivalent location,  $1.1 \mu\text{m}$  downstream to the shock front.

(a)			
$(\varkappa_x, \varkappa_{\perp})$	(1758., 1.40)	(1758., 5.26)	(1758., 131.5)
$\sigma_0^{-1} (10^{-5})$	15.7	15.7	8.06
$\sigma_{\text{AT}}^{-1} (10^{-5})$	15.2	15.2	7.87
(b)			
$(\bar{\lambda}_x, \bar{\lambda}_{\perp}) (\mu\text{m})$	(0.080, 100.)	(0.080, 26.6)	(0.080, 1.06)
$\bar{\sigma}_{\text{AT}}^{-1} (\text{ps})$	0.22	0.22	0.11

<sup>a</sup>See Supplemental Material, Sec. I.B.

Corresponding data obtained in connection with a simulation of a chosen ICF capsule implosion [33] are given in

Table I(b). The associated figures are indicative of characteristic lengths of perturbations that are susceptible to yield transient growth. The perturbations presently identified are in the tens of nanometers in the longitudinal (or radial) direction and within the range 1–100 microns in the transverse (or azimuthal) direction, corresponding for the chosen capsule to Legendre modes ranging from 60 to 6000. These features are compatible with characteristic sizes of ablator material inhomogeneities [12]. The corresponding transient growths, with characteristic times in the sub-picosecond range and significant amplifications of the perturbation norm (event A, Fig. 3), result from the constructive interaction between the localized entropy and acoustic waves that dominate the optimal-growth initial conditions (4) [event A, Figs. 4(a–d)]. The

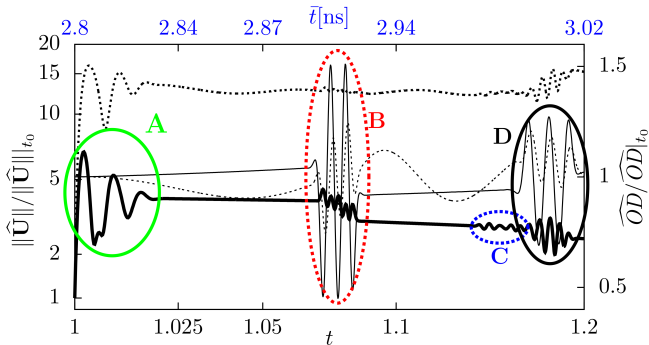


FIG. 3: Amplification of the perturbation norm,  $\|\hat{\mathbf{U}}\|/\|\hat{\mathbf{U}}\|_{t_0}$ , (thick lines—left axis) and of the optical depth perturbation,  $\widehat{\text{OD}}/\widehat{\text{OD}}|_{t_0}$  (thin lines—right axis), for initial conditions Eq. (4) at  $x_* = -0.06$ , with  $\varkappa_x = 1758.$ ,  $\varkappa_\perp = 1.40$  (solid) or  $\varkappa_\perp = 131.5$  (dash). Remarkable events in the evolution of  $\|\hat{\mathbf{U}}\|$  are identified by letters A to D.

ensuing perturbation dynamics proceed from further mutual interactions of these waves [events A and C, Figs. 3 and 4(a–c)], their propagation [Figs. 4(b,c,d)], and interactions with the ablation layer [event B, Figs. 3 and 4(a,b,d)] and shock front [event D, Figs. 3 and 4(a,b)]. The perturbation of the longitudinal optical depth, a quantity used for detecting hydrodynamic disturbances in ICF flow experiments [34], is notably insensitive to the transient growth, varying only when waves interact with the ablation growth and shock front (events B and D, Fig. 3). This insensitivity and the growth time scales, way below current experimental measurement capabilities, make the direct detection of such fast amplification dynamics most unlikely in practice. Ablator materials with bulk inhomogeneities, such as those used in the experiments of Ref. [12], are likely to induce constructive interactions of fluid waves since such inhomogeneities trigger emissions by the shock front (ablation layer) of acoustic and entropy (respectively, acoustic) fluctuations. Simulations with surface roughness alone could not explain the levels of shock-front non-uniformities that were ob-

served in these experiments. Simulations modeling ablator bulk inhomogeneities, due to their computational cost, were not undertaken by that time and have been performed only once since then [5], their results showing enhanced shock-front perturbations. However the leading mechanisms responsible for such perturbation levels are still uncertain and cannot be unraveled on the sole basis of available experimental and simulation data. The present transient growth mechanism is potentially one of them, contributing to perturbation amplification in the compression region and the ablation layer, and thus to an enhanced seeding of ablative Rayleigh–Taylor modes for the subsequent acceleration stage of a capsule implosion [35]. Assessing the importance of this mechanism in capsule implosions requires however experimental diagnostics and/or detailed analyses of high-fidelity simulations that have yet to come.

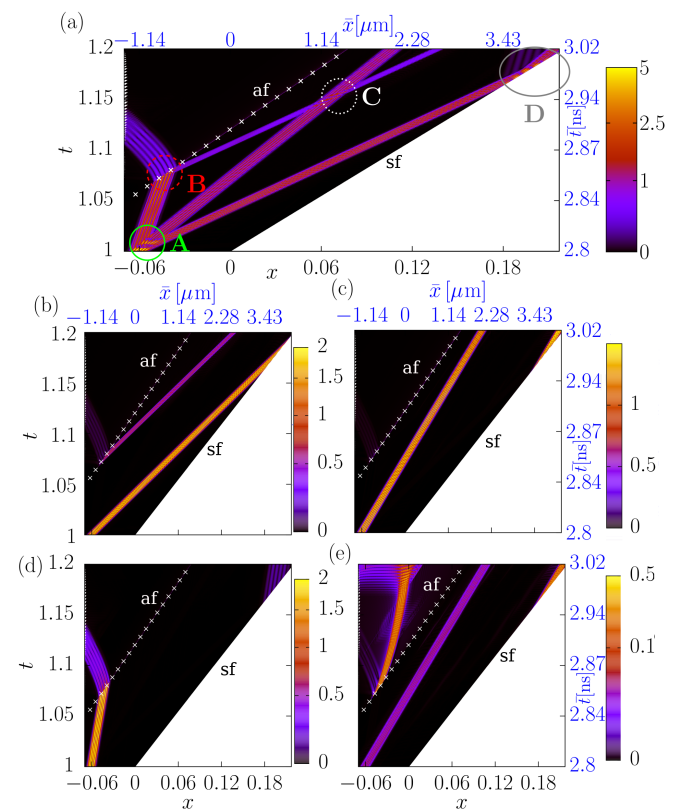


FIG. 4: Evolution of  $\hat{\mathbf{U}}$  in the compression region for initial conditions Eq. (4) at  $x_* = -0.06$ , in the case  $(\varkappa_x, \varkappa_\perp) = (1758, 1.40)$ . Same conventions as in Fig. 1 with shock (sf) and ablation (af) front trajectories. (a) Local Euclidean norm. Components (absolute value) in longitudinal pseudo-characteristic variables [22]: (b) forward and (d) backward acoustic waves, (c) entropy waves. (e) Transverse potential vorticity. Labeled circles in (a) relate to the events identified in Fig. 3.

This Letter brings the first evidences of non-modal effects in the stability of an ablation flow related to ICF. In effect, local transient growth of perturbations may occur

in flow regions that are stable according to the classical method of normal modes. The identified mechanism of transient growth is intrinsic to compressible fluid motion and thus generic to any ICF ablation flow. This mechanism puts forth the possibility, in an ablator with material inhomogeneities, of fast perturbation amplifications, not directly detectable by existing experimental diagnostics but contributing to perturbation enhancement. Such amplifications, compatible with trends observed in inhomogeneous ablator experiments and simulations, could induce transitions to perturbation nonlinear regimes earlier than foreseen by modal stability analysis. Global non-modal stability analyses and high-fidelity simulations would at least be needed to investigate such a possibility. More generally these findings call for applying methods of non-modal stability theory to ICF implosions so as to establish on firmer grounds their predictions, thus reducing uncertainties thereof.

---

\* gregoire.varillon@polytechnique.edu

---

\* gregoire.varillon@polytechnique.edu

- [1] S. Atzeni and J. Meyer-ter-Vehn, *The physics of inertial fusion* (Oxford University Press, Oxford, U.K., 2004).
- [2] S. E. Bodner, Phys. Rev. Lett. **33**, 761 (1974).
- [3] J. D. Lindl and W. C. Mead, Phys. Rev. Lett. **34**, 1273 (1975).
- [4] J. Lindl et al., Phys. Plasmas **21**, 020501 (2014).
- [5] B. M. Haines et al., Phys. Plasmas **26**, 012707 (2019).
- [6] D. S. Clark et al., Phys. Plasmas **26**, 050601 (2019).
- [7] V. Bychkov et al., Prog. Energy Combust. Sci. **47**, 32 (2015).
- [8] P. J. Schmid, Annu. Rev. Fluid Mech. **39**, 129 (2007).
- [9] Y. Aglitskiy et al., Phil. Trans. R. Soc. A **368**, 1739 (2010).
- [10] K. S. Raman et al., Phys. Plasmas **21**, 072710 (2014).
- [11] V. A. Smalyuk et al., Phys. Plasmas **22**, 072704 (2015).
- [12] S. J. Ali et al., Phys. Plasmas **25**, 092708 (2018).
- [13] S. W. Haan et al., Phys. Plasmas **22**, 032708 (2015).
- [14] P. J. Schmid and D. S. Henningson, *Stability and transition in shear flows* (Springer, New-York, 2001).
- [15] L. N. Trefethen et al., Science **261**, 578 (1993).
- [16] R. Marshak, Phys. Fluids **1**, 24 (1958).
- [17] F. Abéguilé et al., Phys. Rev. Lett. **97**, 035002 (2006).
- [18] C. Boudesocque-Dubois et al., J. Fluid Mech. **603**, 151 (2008).
- [19] J.-M. Clarisse et al., J. Fluid Mech. **848**, 219 (2018).
- [20] J.-M. Clarisse et al., J. Fluid Mech. **609**, 1 (2008).
- [21] C. C. Cowen and E. Harel, *An effective algorithm for calculating the numerical range* (1995), URL <https://www.math.iupui.edu/~ccowen/Downloads/33NumRange.pdf>.
- [22] G. Varillon et al., Phys. Rev. E **101**, 043215 (2020).
- [23] D. Mihalas and B. W. Mihalas, *Foundations of radiation hydrodynamics* (Oxford University Press, Oxford, 1984).
- [24] See Supplemental Material, Sec. I.
- [25] See Supplemental Material, Sec. II.
- [26] See Supplemental Material, Sec. II.
- [27] See Supplemental Material, Sec. III.
- [28] Here, the chosen global perturbation norm is defined after the scalar product  $\langle \widehat{\mathbf{U}}, \widehat{\mathbf{V}} \rangle = \frac{1}{2} \int_0^{m_{sf}} \rho^{-1} \widehat{\mathbf{U}}^\dagger \widehat{\mathbf{V}} dm$ .
- [29] See Supplemental Material, Fig. 1(c).
- [30] See Supplemental Material, Fig. 1(b).
- [31] See Supplemental Material, Sec. IV A.
- [32] See Supplemental Material, Sec. II.
- [33] See Supplemental Material, Sec. I.B.
- [34] Hydrodynamic disturbances are classically detected in ICF through measurements of optical depth perturbation [10], presently amounting to  $\widehat{\mathcal{O}}\widehat{\mathcal{D}} = \int_0^{m_{sf}} \rho^{-1} (\kappa_\rho \widehat{\rho} + \kappa_T \widehat{T}) dm + [\partial_x \kappa \widehat{x}]_{es}^{sf}$ , where  $\kappa = 4 \rho^\mu T^{3-\nu}$  is the fluid opacity [23], and  $\widehat{x}_{es|sf}$ , the deformation of the external surface/shock front.
- [35] See Supplemental Material, Sec. IV B.